Proceedings of the 20th International Conference on Soil Mechanics and Geotechnical Engineering– Rahman and Jaksa (Eds)

Simulation of gentle pile driving (GDP) using the Material Point Method

Simulation de Gentle Pile Driving (GDP) avec l'utilisation de la méthode du point de matériau

Mario Martinelli, Vahid Galavi and Ahmed Elkadi
Deltares, The Netherlands, mario.martinelli@deltares.nl

ABSTRACT: Monopiles are the most commonly used foundations for offshore wind turbines in the North Sea, mainly in relatively shallow waters. The dominant method used to drive monopiles into the seabed is hydraulic impact piling (hammering), which produces high-noise levels emitted during pile driving. Recently, a novel pile installation method has been developed in the Netherlands during the project Gentle Driving of Piles (GDP), and one of the advantages is the reduction of the emitted noise during installation. Over the last decade, Deltares has further developed the Material Point Method (MPM) and optimized it for numerically simulating the full installation process of monopiles. In this paper, MPM is used to simulate the installation of open-ended monopiles using the GDP method. The numerical simulations will focus on an idealized soil condition where the relevant effects of such an innovative technique will be analyzed and compared against other installation methods such as impact-hammering and jacking.

RÉSUMÉ : Les monopiles sont les fondations les plus couramment utilisées pour les éoliennes offshore en mer du Nord, principalement dans les eaux relativement peu profondes. La méthode dominante utilisée pour enfoncer les monopiles dans le fond marin est l'empilement hydraulique (martelage), qui produit des niveaux de bruit élevés émis pendant le battage des pieux. Récemment, une nouvelle méthode d'installation de pieux a été développée aux Pays-Bas dans le cadre du projet Gentle Driving of Piles (GDP), et l'un des avantages est la réduction du bruit émis lors de l'installation. Au cours de la dernière décennie, Deltares a développé la méthode du point matériel (MPM) et l'a optimisée pour simuler numériquement le processus d'installation complet des monopiles. Dans cet article, MPM est utilisé pour simuler l'installation de monopiles ouverts à l'aide de la méthode GDP. Les simulations numériques se concentreront sur une condition du sol idéalisée où les effets pertinents d'une telle technique innovante seront analysés et comparés à d'autres méthodes d'installation telles que le martelage par percussion et le vérinage.

KEYWORDS: GDP, MPM, monopiles, installation effects, offshore wind.

1 INTRODUCTION

Monopiles are the most commonly used foundations for offshore wind turbines in the North Sea to date. The dominant method used to drive monopiles into the seabed is impact hammering. One of the main drawbacks of this technique is the high-noise levels emitted during pile driving and the high impact loads on the monopiles induced by hammer strikes. The earlier leads to costly mitigation measures and limited installation time during the year and the latter to heavier design. Recently, a novel pile installation method has been developed in the Netherlands during the project Gentle Driving of Piles (GDP). The method has been successfully tested on scaled monopiles in the Maasvlakte 2, Rotterdam, The Netherlands [Metrikine et al. 2020]. The GDP method is based on the simultaneous application of low-frequency and high-frequency vibrators exciting two independent modes of motion on the monopiles (axial and/or torsional modes). One of the anticipated advantages of this new method is related to the reduction of the emitted noise during installation.

Over the last decade, Deltares has further developed and improved the Material Point Method (MPM) to become a suitable numerical tool for simulating the full installation process of monopiles, where large deformations are severely mobilized into the soil next to the structure with highly complex (dynamic) soil-structure-water interaction [Galavi et al., 2019]. This allows for a better assessment of the state of stress around the pile due to installation since the soil state changes considerably during this process [Nguyen et al., 2016]. Next to assessing the soil state during and after installation, this method can be used as well for drivability and optimization studies.

In this paper, the Deltares MPM code is used to simulate the installation of open-ended steel piles (monopiles), which are installed using the GDP method. The numerical simulations focused on an idealized soil condition where the relevant effects of such an innovative technique are analyzed and further compared against other more classical installation methods such as impact-hammering and jacking.

2 2D-AXISYMMETRIC MPM WITH ROTATIONAL DOF

The 2D axisymmetric formulation with a rotational degree of freedom is a generalization of the already available formulation presented in Galavi et al. (2018).

The strain tensor in a rotational axisymmetric problem is defined as:

$$\varepsilon_{rr} = \frac{\partial u_r}{\partial r} \tag{1}$$

$$\varepsilon_{yy} = \frac{\partial u_y}{\partial y} \tag{2}$$

$$\varepsilon_{\theta\theta} = \frac{u_r}{r} \tag{3}$$

$$\gamma_{ry} = 2\varepsilon_{ry} = \left(\frac{\partial u_r}{\partial y} + \frac{\partial u_y}{\partial r} \right) \tag{4}$$

$$\gamma_{y\theta} = 2\varepsilon_{y\theta} = \frac{\partial u_\theta}{\partial y} \tag{5}$$

$$\gamma_{r\theta} = 2\varepsilon_{r\theta} = \left(\frac{\partial u_\theta}{\partial r} - \frac{u_\theta}{r} \right) \tag{6}$$

In which u_r, u_y and u_θ are the displacements in the cylindrical coordinate system corresponding to r (radial coordinate), y (vertical coordinate) and θ (circumferential coordinate).

In conventional axial axisymmetric problems, in which there is no rotation θ around the axis of symmetry, the displacements u_θ are zero and the above six non-zero strain components reduce to four non-zero strain components (Galavi et al., 2018).

In finite element or MPM, the strains are related to the nodal displacements ui, with the B matrix as follows

$$\boldsymbol{\varepsilon} = \mathbf{B}\mathbf{u}_i \tag{7}$$

$$\mathbf{B}_i = \mathbf{L}\mathbf{N}_i = \begin{bmatrix} \partial N_i(x)/\partial r & 0 & 0 \\ 0 & \partial N_i(x)/\partial y & 0 \\ N_i(x)/r & 0 & 0 \\ \partial N_i(x)/\partial y & \partial N_i(x)/\partial r & 0 \\ 0 & 0 & \partial N_i(x)/\partial y \\ 0 & 0 & \partial N_i(x)/\partial r - N_i(x)/r \end{bmatrix} \quad (8)$$

Therefore, the internal force is expressed for the standard MPM (Sulsky et al., 1994) as:

$$f_i^{int} = \sum_{MP=1}^{n_{vp}} B_i^T \left(x_{MP}\right) \sigma_{MP} \Omega_{MP} \quad (9)$$

where x_{MP}, σ_{MP} and Ω_{MP} are the position, stress and int egration weight of the material point, respectively.

The discretized form of the momentum balance equation of the solid phase for a generic node i of the computational mesh is written as follows:

$$\boldsymbol{f}_i^{ext} - \boldsymbol{f}_i^{\text{int}} = M_i \boldsymbol{a}_i \quad (10)$$

where, M_i, $\boldsymbol{f}^{ext}$ and $\boldsymbol{f}^{int}$ are the nodal values of the mass matrix, external force and internal force.

For soil-structure-interaction problems, the contact algorithm proposed by Bardenhagen et al. (2000) is used to model separation and sliding between the soil and structure by means of the Coulomb failure criterion.

An explicit time integration scheme (Sulsky et al., 1994) is used in the MPM code with optimization options to reduce the computational time, as discussed in Martinelli and Galavi (2020).

The 2D rotational axisymmetric formulation is validated by simulating the torque of an open-ended pile. The geometry is shown in Figure 1a. The width and the height of the model are 1 m. The pile thickness is 0.2 m and is placed exactly in the middle of the geometry. The radius of the internal and external shaft surface is then 0.4 m 0.6 m, respectively. The length of the pile is 0.5 m. Linear elastic material is considered for both pile and soil with a relatively high stiffness of 100 MPa. The Poisson's ratio is set to 0. An adhesive contact is assumed between the pile and soil with and adhesion τ_c = 10 kPa. A constant out-of-plane rotation with an angular velocity of 0.02 rad/s is applied to the pile in a dynamic analysis with a duration of 1 second.

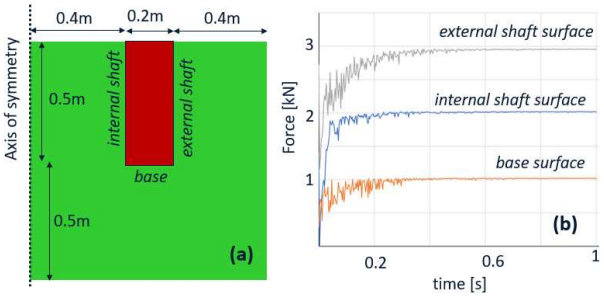

Figure 1: Validation of the 2D rotational axisymmetric formulation: (a) geometry of the numerical model; (b) reaction forces along the pile surfaces.

By integrating the adhesion along the internal, external and base of the pile, the analytical values of the quasi-static reaction forces are:

$$F_{internal} = rh\tau_c = 0.4 \times 0.5 \times 10 = 2\,kN/rad \quad (11)$$

$$F_{external} = rh\tau_c = 0.6 \times 0.5 \times 10 = 3\,kN/rad \quad (12)$$

$$F_{base} = \int_{r_1}^{r_2} r\tau_c dr = \frac{1}{2}10\left(0.6^2 - 0.4^2\right) = 1\,kN/rad \quad (13)$$

The calculated reaction forces in the MPM model are presented in Figure 1b and, at steady-state condition (i.e. after 0.4 s of simulation), they are very close to the analytical solution (Eq. 11-13).

3 INSTALLATION OF OPEN-ENDED MONOPILE

An open-ended pile is considered for this study, with the geometry described in Table 1. The pile is installed in an ideal dry and homogeneous medium-dense sand deposit.

Three different installation methods are simulated: jacked, impact driven and GDP.

The jacked installation is simulated by applying a constant velocity (2 cm/s) to the entire pile body.

The impact-drive installation is simulated by applying a distributed force at nodes of the pile head. The shape of the force in time is described as follows:

$$F(t) = \begin{cases} F_{\max} \sin\left(\dfrac{\pi t}{t_1}\right) & for\ t \le t_1 \\ 0 & for\ t > t_1 \end{cases} \quad (14)$$

The values of F_{max} and t_1 are listed in Table 2, which approximately correspond to the load generated by a falling mass of 4.5 Mg with an energy of 25 kJ.

The GDP simulations are simulated applying only torsional harmonic loading as described in Table 3. The body weight of the shaker is also applied as static load at the pile head.

Table 1: Pile dimensions

Parameter	Value	Description
L [m]	14.0	Length
D [m]	0.746	Diameter
t [m]	0.0159	Thickness

Table 2: Impact force characteristics

Parameter	Value	Description
F_{max} [kN/rad]	750	Max force
Δt	0.85	Blow interval
t_1 [s]	0.005	Impulse time

Table 3: torsional loading characteristics (induced by the GDP shaker)

Parameter	Value	Description
M_{max} [kNm]	414.5 / 829	Max. torque moment
F_y [kN/rad]	8	Static vertical force
f [Hz]	60	Frequency

The numerical model

The numerical model is illustrated in Figure 2. It is a 2D axisymmetric model with rotational degree of freedom, as described in Section 2. The width of the model is 5 m and the thickness of the sand layer is 10 m. All degrees of freedom of nodes on lateral boundaries are fixed in normal direction.

The soil and pile properties are listed in Table 4. The pile is modeled with a linear elastic material. To reduce the computational time, the rigid body formulation is used to simulate the pile response where the motion is calculated only at the DoF (Degree of Freedom) of the center of mass and no wave propagation is simulated. The soil is modeled using a double hardening constitutive model (Hardening Soil model) (Schanz et. al., 1999) and the model parameters are listed in Table 5. The soil

model with the given material parameters reproduces existing oedometer test results of medium-dense sands, and the simulation of a CPT in MPM at σ'_{v0} = 50 kPa provides a cone resistance of approximately 12 MPa, which results in the same range of values measured in the field in case of medium-dense sand (Martinelli and Galavi, 2020).

Quadrilateral elements with linear shape functions are used in the simulations. To mitigate volumetric locking, the B-bar approach is performed at every computational step (Hughes, 2000). A sufficiently large number of material points is used to avoid the formation of numerical fracture (empty element) during the pile penetration.

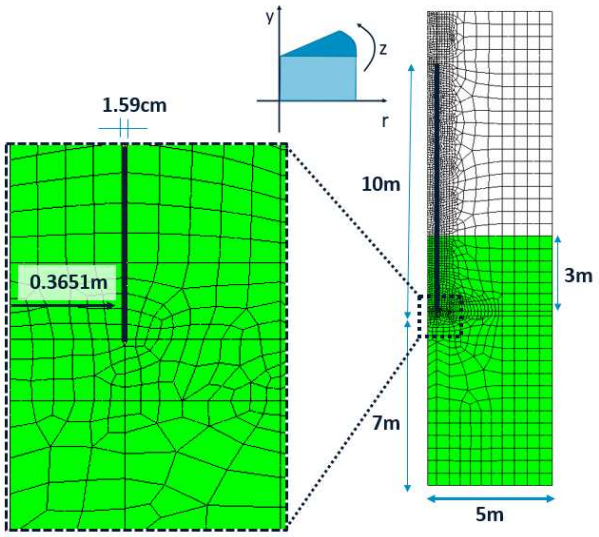

Figure 2: Geometry of the numerical model with the close-up view of the tip.

Table 4: Soil and pile properties

Parameter	Value	Description
Gs [-]	2.65	Specific gravity
n [-]	0.375	Initial soil porosity
ρ [kg/m^3]	8000	Pile density
E [GPa]	220	Young's modulus of pile
ν [-]	0.0	Poisson's ratio of pile

Table 5: Hardening Soil model parameters for the soil

Parameter	Value	Description
E_{50}^{ref} [kPa]	44000	reference triaxial secant stiffness
E_{oed}^{ref} [kPa]	44000	reference oedometer stiffness
E_{ur}^{ref} [kPa]	132000	reference Young's modulus for unloading/reloading
m [-]	0.47	power for stress dependency of stiffness
ν [-]	0.2	unloading/reloading Poisson's ratio
$k_{0,NC}$ [-]	0.5	Earth pressure coefficient for normally consolidated soil
R_f [-]	0.91	Failure ratio
p_{ref} [kPa]	100	Reference mean stress
φ'_u [deg]	37.5	Ultimate friction angle
ψ_u [deg]	0.0	Ultimate dilation angle

The contact algorithm (Bardenhagen et al., 2000) is defined for all surfaces of the structure. In order to improve the accuracy of the calculation, the moving mesh concept is used, i.e. the mesh is moved during the simulation to keep the same contact surface between the pile and soil (Al-Kafaji, 2013). Moreover, the accuracy of the numerical solution along the contact nodes was further improved as discussed in Martinelli and Galavi (2020). A contact friction angle of 21.8 degrees is used in all simulations, which results in a friction coefficient equal to 0.4.

The pile has an initial embedment of 3 m. The stress field is initialized using a K_0-procedure, assuming a K_0 value of 0.5. Before the installation, the system reaches the equilibrium via a damped dynamic self-weight simulation.

Numerical results

The numerical results of the three types of installation processes are illustrated in Figure 3 to Figure 7, expressed in terms of evolution of contact reaction forces with penetration. The reaction forces are calculated as the summation of all contact forces along the three surfaces: tip, internal shaft and external shaft. The figures show the results for the first 0.6 m of penetration.

The jacked installation is characterized by the development of high stresses inside the pile, which induce large radial outward forces on the internal shaft and at the pile tip (Figure 3). These high stresses result into high strength along the interface on the interior surface of the pile (Figure 4), where the reaction forces (F_y) in the penetration direction are approximately 4 times larger than the corresponding ones on the external shaft. Large tip resistance is also computed. The friction ratio (F_y/F_r) illustrated in Figure 5 shows that, for both internal and external shafts, the ratio reaches the maximum value of 0.4, i.e. sliding take place along the contact and no plug formation occurs.

The impact-driven installation is characterized by high peak reaction forces, due to the large impulse loads and the consequently soil-structure interaction. It is observed in Figure 3 and Figure 4, that the radial and vertical reaction forces generated during the impact-driven installation, at the tip and at the external shaft, tend to follow the curve for jacked installation. On the contrary, the response along the internal shaft is much lower, where the peak values of F_r (and F_y) do not exceed approximately the 30% of those of the jacked installation. No plug formation occurs also in this installation method, as on both the internal and external shaft, the friction ratio (F_y/F_r) (Figure 5) reaches the maximum allowable value of 0.4 during the downward displacement.

The GDP installation is characterized by torsional harmonic loading at high frequency. The results presented in Figure 3 to Figure 6 refer to the lowest moment torque value in Table 3 (i.e. Mmax = 414 kN m/rad). Higher loading values affect the penetration rate but not the evolution of the reaction forces with depth; for this reason, they are not included in the figures.

Along the shaft (both internal and external), the GDP installation induces radial forces which are similar to those of the impact-driven case. The main difference is at the pile tip, where the radial reaction force is almost zero. This means that during the GDP installation, in the soil close to the pile tip, there is no appreacable difference in the stresses field between the inner side and outer side of the pile.

The beneficial characteristic of the GDP installation is that the out-of-plane shear stresses induced by the harmonic torque decrease the overall bearing capacity of the pile, facilitating the installation. This effect is illustrated in Figure 4, where reaction forces at the tip and along the shafts are much lower compared to other installation methods. The vertical friction ratio F_y/F_r (Figure 5) decreases for GDP case to values below 0.2, as if the "apparent" contact friction angle gets lower during the installation. This effect is confirmed by the total friction ratio F_{total}/F_r (Figure 6) which reaches the maximum allowable value of 0.4 during shaking, along both shaft surfaces.

Figure 7 shows the evolution in time of pile penetration for all installation methods. The curve show that impact-driven installation is the fastest method that reaches 0.6m of penetration. It is worth noticing that this is not a general conclusion, but it is only valid for this example with a given geometry of the soil and pile, where specific values for external loads (Table 2 and Table 3) are selected, which correspond to different energies.

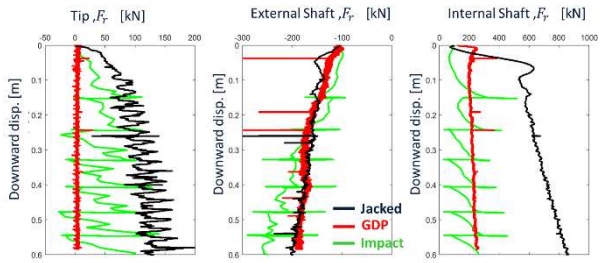

Figure 3: Radial forces (F_r) on the tip, external shaft and internal shaft. Positive value if the force is directed according to the datum of Figure 2.

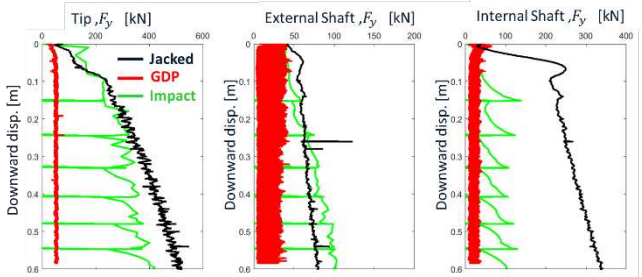

Figure 4: Vertical forces (F_y) on the tip, external shaft and internal shaft. Positive value if the force is directed according to the datum of Figure 2.

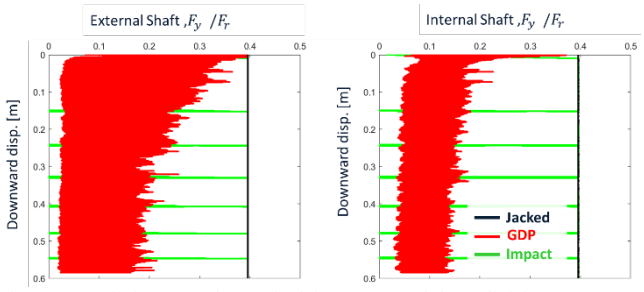

Figure 5: Ratio between the vertical force (F_y) and the radial force (F_r).

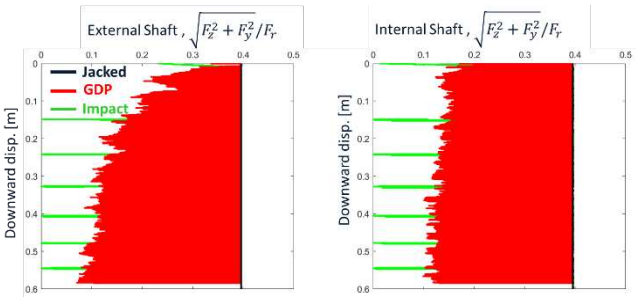

Figure 6: Ratio between the total shear force and the radial force (F_r)/

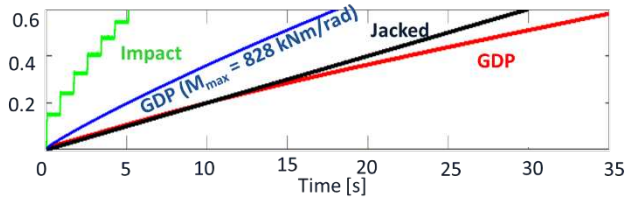

Figure 7: pile penetration in time for all installation methods.

Figure 8, Figure 9 and Figure 10 show the soil shear stress distribution for all installation methods at 0.6 m of penetration. Figure 8 shows results for jacked installation, where large stresses are computed below the tip and inside the pile, due to considerable arching effect. Figure 9 illustrates the stress field right before the next blow, which shows large values mainly below the pile tip. It is worth noticing that shear stresses have mainly the same sign, explaining the large radial force induced during the installation.

The stress field during GDP installation is shown in Figure 10, where relatively low shear stresses are mobilized during cyclic loading. It is worth mentioning in this case, that below the pile tip, the distribution of shear stresses is symmetric between inner and outer side of the pile. This explains the negligible radial force computed during the installation.

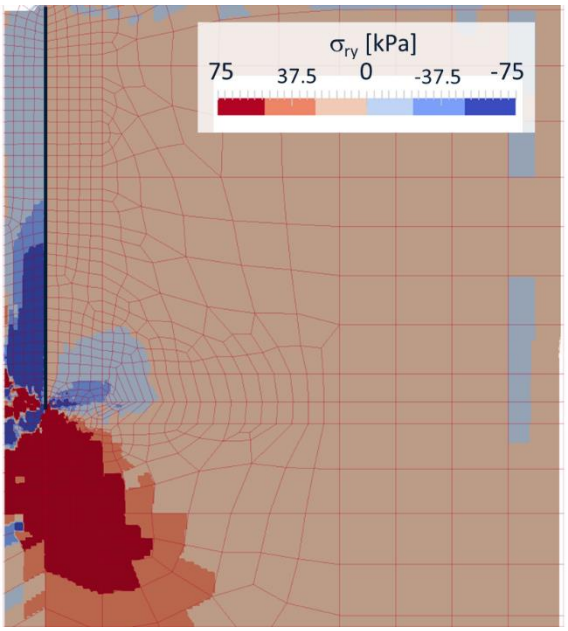

Figure 8: Jacked installation. Pile penetration of 0.6m. Distribution of shear stresses (σ_{ry}) in the soil.

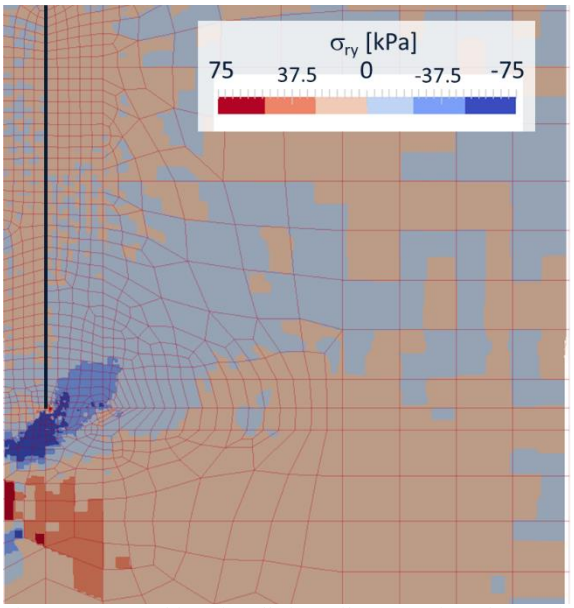

Figure 9: Impact driven installation. Pile penetration of approximately 0.6m. Distribution of shear stresses (σ_{ry}) before the next blow.

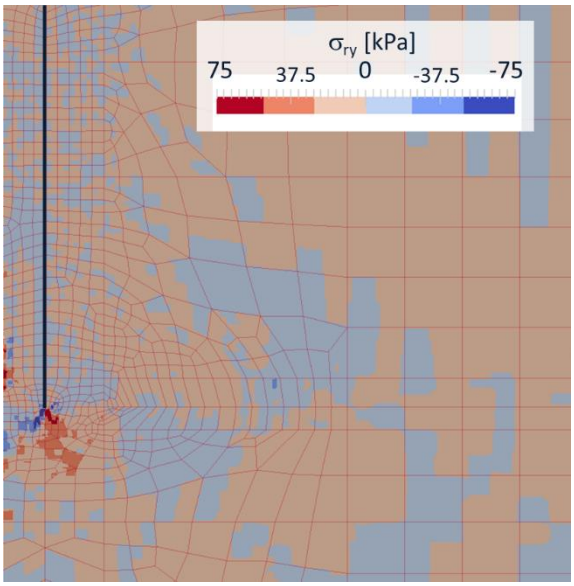

Figure 10: GDP installation. Pile penetration of approximately 0.6m. Distribution of shear stresses (σ_{ry}) during GDP loading.

2 CONCLUSIONS

In this paper, the Deltares MPM tool for numerical simulation of pile installation is further extended by including the rotational degree of freedom in an existing 2D axisymmetric formulation in order to achieve efficient calculation of monopiles installed by means of GDP technique. The numerical simulations focus on an idealized soil condition where the relevant effects of such an innovative technique are analyzed and compared against other installation methods such as impact-hammering and jacking.

It is worth noticing that the numerical simulations are performed using a state-independent constitutive model under drained conditions, which is not optimal for cyclic loading, but it is simple enough to highlight the essential aspects of the challenging installation methods. In future, a more advanced constitutive model will be used to properly simulate soil response under cyclic loading under undrained or partially drained conditions, especially for soils underwater where considerable excess pore pressures develop.

3 ACKNOWLEDGEMENTS

This paper is associated with the GDP project in the framework of the GROW joint research program. Funding from "Topsector Energiesubsidie van het Ministerie van Economische Zaken" under grant number TEHE117100 and financial/technical support from the following partners is gratefully acknowledged: Royal Boskalis Westminster N.V., CAPE Holland B.V., Deltares, Delft Offshore Turbine B.V., Delft University of Technology, Eneco Wind B.V., IHC IQIP B.V., SHL Offshore Contractors B.V., Shell Global Solutions International B.V., Sif Netherlands B.V., TNO, and Van Oord Offshore Wind Projects B.V.

4 REFERENCES

Al Kafaji I. 2013. Formulation of a dynamic material point method (MPM) for geomechanical problems. PhD thesis Univ. of Stuttgart, Germany.

Bardenhagen SG, Brackbill JU, Sulsky D. 2000. The material-point method for granular materials. *Computer Methods in Applied Mechanics and Engineering* 187:529–541.

Galavi, V., Martinelli, M., Elkadi, A., Ghasemi, P., Thijssen, R., 2019. Numerical simulation of impact driven offshore monopiles using the material point method. *In: Proceedings of the XVII ECSMGE 2019*. https://doi.org/10.32075/17ECSMGE-2019-0758.

Hughes, T. J. 2000. *The Finite Element Method: Linear Static and Dynamic Finite Element Analysis*. Dover Civil and Mechanical Engineering. Courier Corporation.

Martinelli M., Galavi V. 2020. Investigation of the Material Point Method in the simulation of Cone Penetration Tests in dry sand. *Computers and Geotechnics* 130.

Metrikine A.V., Tsouvalas A., Segeren M.L.A., Elkadi A.S.K., Tehrani F.S., Gómez S., Atkinson. R, Pisano F., Kementzetzidis E., Tsetas A., Molenkamp T., van Beek K. and De Vries P. 2020. GDP: A New Technology for Gentle Driving of (Mono)Piles, *Proc. 4th International Symposium on Frontiers in Offshore Geotechnics ISFOG 2020,* Austin, Texas, USA.

Schanz, T., Vermeer, P.A., Bonnier, P.G., 1999. The hardening soil model: formulation and verification. In: *Proceedings of the International Symposium Beyond 2000 in Computational Geotechnics*, Amsterdam, The Netherlands, pp. 281–296. https://doi.org/10.1201/9781315138206-27.

Sulsky D., Chen Z., Schreyer H.L. 1994. A particle method for history-dependent materials. *Comput. Meths. Appl. Mech. Engrg*. 118, 179–196.